A two-layer depth-averaged model of dry granular material for dam-break flows

L. SARNO[1], A. CARRAVETTA[2], R. MARTINO[2], Y. C. TAI[3], M. N. PAPA[1]
[1]Department of Civil Engineering
University of Salerno
Via Giovanni Paolo II, 132, Fisciano, 84084
ITALY
lsarno@unisa.it, mnpapa@unisa.it, http://www.unisa.it/dipartimenti/diciv/lidam/en/index

[2]Department of Civil, Architectural and Environmental Engineering
University of Napoli Federico II
Via Claudio, 21, Napoli, 80125
ITALY
armando.carravetta@unina.it, riccardo.martino@unina.it, http://dicea.dip.unina.it/en/home/?lang=en

[3]Department of Hydraulic and Ocean Engineering
National Cheng Kung University
Tainan, 70101
TAIWAN
yctai@mail.ncku.edu.tw, http://www.hyd.ncku.edu.tw/en/

Abstract: In this work, we propose a two layer depth-averaged model to describe the propagation up to the deposition of granular avalanches. The model is derived in Cartesian coordinates under the assumption of long wave approximation. The two layers are supposed to follow to different flow regimes. A friction-collisional beaviour is assumed in the upper layer, while a purely frictional behaviour holds in the lower one. The model is numerically integrated through using a finite volume scheme. Since the resulting PDE system is only conditionally hyperbolic, a special treatment, involving the addition of an extra momentum flux across the interface between the layers, is implemented in the numerical scheme. The key features of this approach are illustrated by some numerical tests.

Key-Words: depth-averaged models, granular flows, two-layer models, dam-break, avalanche, debris flows

1 Introduction

Granular avalanches and debris flows are hazardous phenomena, characterized by the fast motion of granular matter embedded in an ambient fluid. A proper description of the propagation stages of these events, from the onset to the deposit, is crucial to predict run-out distances and properly delimit the endangered areas. Recently, several efforts have been made to better understand the dynamics of granular flows and solid-liquid mixtures from both theoretical and experimental viewpoints (e.g. [4,5,13,21,23,24,26,33]). Yet, the dynamics of granular matter is found to exhibit different regimes that are difficult to be described by a unique constitutive law. An effective approach to describe the propagation of granular flows is represented by depth-averaged hydrodynamic models, that treat the granular material as a continuum and allow a straightforward and fast numerical integration. A popular model of this kind is represented by the Savage-Hutter (SH) model [29], in which a Mohr-Coulomb behavior is used for internal and basal stresses. Several laboratory experiments have showed its capability to capture the main features of granular avalanches over relatively smooth beds (e.g. [12]). However, in the case of no-slip bottom boundary condition, the reliability of the SH theory is limited by the constant distribution assumed for both flow velocity and bulk density profiles (e.g. [22,26]). In the presence of no-slip bottom boundary condition, some works [1,9] experimentally reported the existence of two distinct regions with different velocity and volume fraction profiles in the same cross section. These findings suggest that two different flow regimes take place. In the lower zone of the flow, the momentum transfer is expected to

ISBN: 978-960-474-376-6

be only due to grain friction, while in the upper one also momentum collision mechanisms occur. In case of rough bottom surface, a slow creeping flow is found in the lower zone below a surface flow zone [14]. Similarly, collapses of granular columns, experimentally studied in [16,18], exhibit a slow lower layer that reaches a state of rest in advance with respect to the upper surface flow. Discrete element numerical simulations (DEM) have been employed to increase the insight into collapses of granular columns (e.g. [15,30]) and bring further evidence of the aforementioned flow regime stratification. Mangeney et al. [20] tried to describe the collapse of granular material through using a minimal depth-averaged model with basal Coulomb friction. The degree of agreement with experimental data is very good for small initial aspect ratios of the granular column but the model is found to be less reliable in case of high initial aspect ratios, where the run-out distances are noticeably overestimated. These findings suggest that more information is needed to properly describe the propagation of granular flows in case of no-slip bottom boundary conditions and classical depth-averaged models seem to be less suitable. Aside from fully three-dimensional models, an alternative approach is represented by multi-layer depth-averaged models (e.g. [2]). Such models exhibit a good numerical efficiency and give a better insight into the velocity distribution along the flow depth with respect to classical depth-averaged models. Recently, the employment of these models in the contexts of fluid mechanics and hydraulic engineering has been noticeably increased (e.g. [3,6,8,19]). Nevertheless, this kind of models show an important mathematical issue, as they are only conditionally hyperbolic. As a result, numerical methods are not yet mature as in classical depth-averaged models.

By following the approach proposed by [25], in this work we present a one-dimensional two-layer model, written in Cartesian coordinates, to describe the propagation of granular avalanches on rough beds. Particular attention is paid to the implementation and description of the numerical scheme. A slight modification of the source terms, with an extra momentum flux at the interface between the layers, to be added if necessary, is proposed in order to guarantee the hyperbolicity of the model. Some numerical tests are performed to show the key features of the model. The numerical results of the two-layer approach are directly compared with a single-layer depth-averaged model with basal Coulomb friction and isotropy of normal stresses. Significant differences in the run-out distances are found and are carefully discussed.

2. Model equations

In this section, we derive the depth-averaged two-layer model in one dimension, similarly to what done in [25] and [27]. With reference to a channelized flow, an orthonormal Cartesian frame of reference is considered, where x-axis is parallel to the channel bed and z-axis points upwards (Fig. 1).

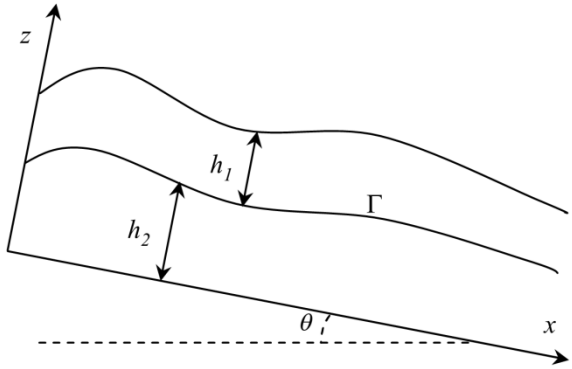

Fig.1 Sketch of the two-layer flow structure.

We regard the dry granular flow as composed of two superimposed flowing layers of depths h_1 and h_2, separated by a sharp interface, Γ, with equation $F_\Gamma(x,z,t) = z - h_2(x,t) = 0$. By indicating the physical quantities in the upper and lower layer with the subscripts "1" and "2", the mass and momentum conservation equations are written as follows

$$\partial_t \rho_\alpha + \mathrm{div}\left(\rho_\alpha \boldsymbol{v}_\alpha\right) = 0, \tag{1}$$

$$\partial_t \left(\rho_\alpha \boldsymbol{v}_\alpha\right) + \mathrm{div}\left(\rho_\alpha \boldsymbol{v}_\alpha \boldsymbol{v}_\alpha^T - \boldsymbol{T}_\alpha\right) = \rho_\alpha \boldsymbol{g}, \quad \alpha \in \{1,2\}, \tag{2}$$

in which ρ represents the bulk density, $\boldsymbol{v}$ is the flow velocity, $\boldsymbol{T}$ is the stress tensor and $\boldsymbol{g}$ is the gravity vector. It is assumed that mass exchanges, M_{flux}, take place between the two layers and, hence, the interface is a non-material surface.

Several experiments showed that the bulk density, ρ, typically increases with distance from free surface (e.g. [9]). In the proposed model we assume, for simplicity, that ρ is constant within each layer and $\rho_1 < \rho_2$. By following [10], the flow velocity, $\boldsymbol{v}$, and $\boldsymbol{T}$ are supposed to be continuous functions within each layer and exhibit a discontinuity across Γ. By using the notation $[[f]]_2^1 = f_{1,\Gamma} - f_{2,\Gamma}$ with $f_{1,\Gamma} = \lim_{z \to h_2 +} f$, $f_{2,\Gamma} = \lim_{z \to h_2 -} f$ and f is any given function, the Rankine-Hugoniot jump conditions for the local mass and momentum conservation read as follows

$$[[\rho\left(\boldsymbol{v} - \boldsymbol{v}_{\mathrm{int}}\right) \cdot \boldsymbol{n}]]_2^1 = 0, \tag{3}$$

$$[[(\rho \boldsymbol{v}(\boldsymbol{v} - \boldsymbol{v}_{\mathrm{int}})^T - \boldsymbol{T})\boldsymbol{n}]]_2^1 = \boldsymbol{0}, \tag{4}$$

ISBN: 978-960-474-376-6

in which $\boldsymbol{v}_{\text{int}}$ is the interface velocity and $\boldsymbol{n}$ is the unit normal vector of Γ. After defining the volume flux across Γ,

$$E_\alpha = M_{flux}/\rho_\alpha = (\boldsymbol{v}_\alpha - \boldsymbol{v}_{\text{int}})\cdot\boldsymbol{n}, \quad \alpha \in \{1,2\}, \tag{5}$$

and some algebraic manipulations Eq. (3) reduces to

$$[[\boldsymbol{v}]]_2^1 \cdot \boldsymbol{n} = -\frac{[[\rho]]_2^1}{\rho_1 \rho_2} M_{flux}. \tag{6}$$

Eq. (6) relates flow velocity and bulk density jumps. Similarly, the momentum jump condition, Eq. (4), is recast to

$$(\boldsymbol{v}_1 - \boldsymbol{v}_2) M_{flux} = (\mathbf{T}_1 - \mathbf{T}_2)\boldsymbol{n}, \tag{7}$$

The x-component of Eq. (7) will be used hereafter as closure equation to calculate M_{flux}. The advantage of using the Rankine-Hugoniot jump condition as closure equation is that it only depends on the constitutive laws of the flowing layers and, thus, no *ad-hoc* calibration of additional parameters is needed. By projecting Eq. (7) on $\boldsymbol{n}$ direction and with the help of Eq. (6), we get the following expression of the normal stress jump at the interface,

$$((\boldsymbol{T}_1 - \boldsymbol{T}_2)\boldsymbol{n})\cdot\boldsymbol{n} = -\frac{\rho_1 - \rho_2}{\rho_1 \rho_2} {M_{flux}}^2. \tag{8}$$

2.1 Depth-averaging

Before depth-averaging the balance equations Eqs. (1)-(2), it is required to define the kinematic and dynamic boundary conditions (KBC and DBC). The KBC at the free surface, $F_f = z - h(x,t) = 0$ with $h = h_1 + h_2$, can be written as

$$\partial_t h + v_{1,x}\partial_x h - v_{1,z} = 0, \tag{9}$$

where $v_{1,x}$ and $v_{1,z}$ are the x and z-component of flow velocity. Since Γ is a non-material surface, the KBC there reads

$$-\partial_t h_2 - v_{\alpha,x}\partial_x h_2 + v_{\alpha,z} = (\boldsymbol{v}_\alpha - \boldsymbol{v}_{\text{int}})\cdot\nabla F_\Gamma, \alpha \in \{1,2\}. \tag{10}$$

Henceforth, we use the over-barred notation to indicate the mean value of a given function f over the flow thickness, viz. for the upper layer

$\overline{f} = 1/h_1 \int_{h_2}^{h_1+h_2} f\, dz$.

By using Eqs. (9)-(10) and with help of Eq. (6), the mass balance equation, depth-integrated in the upper layer, reads

$$\partial_t h_1 + \partial_x\left(\overline{v_{1,x}} h_1\right) = M_{flux}/\rho_1 |\nabla F_\Gamma|. \tag{11}$$

The bottom surface is supposed to be rigid and plain, so that the KBC there is simply given by

$$v_{2,z} = 0. \tag{12}$$

By using KBCs (10)-(12), the depth-integrated mass balance equation of the lower layer reads

$$\partial_t h_2 + \partial_x\left(\overline{v_{2,x}} h_2\right) = -M_{flux}/\rho_2 |\nabla F_\Gamma|. \tag{13}$$

By assuming a traction-free condition at the free surface, the DBC there reads

$$\mathbf{T}_1 \boldsymbol{n} = \mathbf{0}. \tag{14}$$

Analogously to the SH model [29], we assume that the lower layer has a Coulomb-like frictional behavior. Thus, the DBC at the bottom surface can be written as follows

$$\boldsymbol{T}_2\boldsymbol{n} - (\boldsymbol{T}_2\boldsymbol{n}\cdot\boldsymbol{n})\boldsymbol{n} = \text{sgn}(\boldsymbol{v}_{2,t})(-\boldsymbol{T}_2\boldsymbol{n}\cdot\boldsymbol{n})\tan\varphi_B \tag{15}$$

where $\boldsymbol{v}_{2,t} = \boldsymbol{v}_2 - (\boldsymbol{v}_2\cdot\boldsymbol{n})\boldsymbol{n}$ represents the tangential to the bed component of the flow velocity and φ_B is the basal angle of friction. At the interface, two different constitutive relations are defined, as limits from the upper and lower sides of Γ. The shear stress, as limit from the lower side of Γ, is supposed to be purely frictional

$$\boldsymbol{T}_2\boldsymbol{n} - (\boldsymbol{T}_2\boldsymbol{n}\cdot\boldsymbol{n})\boldsymbol{n} = \text{sgn}(\Delta\boldsymbol{v}_t)(-\boldsymbol{T}_2\boldsymbol{n}\cdot\boldsymbol{n})\tan\varphi_{\text{int}}, \tag{16}$$

in which φ_{int} is the angle of internal friction and $\Delta\boldsymbol{v}_t = (\boldsymbol{v}_1 - \boldsymbol{v}_2) - [(\boldsymbol{v}_1 - \boldsymbol{v}_2)\cdot\boldsymbol{n}]\boldsymbol{n}$. At the upper side of Γ, the regime is assumed to be friction-collisional. The shear stress is assumed to be of Voellmy type [34] and can be written as sum of a friction term and a rate-dependent term,

$$\boldsymbol{T}_1\boldsymbol{n} - (\boldsymbol{T}_1\boldsymbol{n}\cdot\boldsymbol{n})\boldsymbol{n} = \text{sgn}(\Delta\boldsymbol{v}_t)\left[k(-\boldsymbol{T}_1\boldsymbol{n}\cdot\boldsymbol{n})\tan\varphi_{\text{int}} + c\rho_2\Delta\boldsymbol{v}^2\right] \tag{17}$$

where k and c are dimensionless parameters. The parameter $k < 1$ is to take into account the decrease of friction due to the density jump across the interface. Substituting (16)-(17) into Eq. (7), the closure equation for calculating the mass flux is fully defined.

With the help of the KBCs, DBCs and the Leibniz rule, the integrated x-component momentum balance equation of the upper layer reads [27]

$$\partial_t\left(\overline{v_{1,x}} h_1\right) + \partial_x\left(\overline{v_{1,x}^2} h_1 - \frac{\overline{t_{1,xx}}}{\rho_1} h_1\right) = v_{1,x,\Gamma}\frac{M_{flux}}{\rho_1}|\nabla F_\Gamma| + \frac{t_{1,xx,\Gamma}}{\rho_1}\partial_x h_2 - \frac{t_{1,xz,\Gamma}}{\rho_1} + h_1 g_x, \tag{18}$$

where the subscript Γ means that the term is evaluated at the interface. Analogously, we obtain the depth-integrated x-momentum balance equation for the lower layer

$$\partial_t\left(\overline{v_{2,x}} h_2\right) + \partial_x\left(\overline{v_{2,x}^2} h_2 - \frac{\overline{t_{2,xx}}}{\rho_2} h_2\right) = -v_{2,x,\Gamma}\frac{M_{flux}}{\rho_2}|\nabla F_\Gamma| - \frac{t_{2,xx,\Gamma}}{\rho_2}\partial_x h_2 + \frac{t_{2,xz,\Gamma}}{\rho_2} - \frac{t_{2,xz,0}}{\rho_2} + h_2 g_x, \tag{19}$$

where the subscript 0 means that the term is evaluated at the bottom surface.

ISBN: 978-960-474-376-6

2.2 Simplifications

Geophysical granular flows are typically thin and long, so that the long-wave approximation can be used to leave non-significant physical quantities out of the model equations [29]. A more rigorous scaling simplification, leading to the same final equations, can be found in [27] where scalings similar to those ones proposed in [32] are employed. Owing to these assumptions, a hydrostatic normal pressure distribution in both layers is derived from the z-component momentum balance equation

$$t_{1,zz}(z) = -\rho_1 g_z (h - z) \tag{20}$$

$$t_{2,zz}(z) = t_{1,zz}(z_i) - \rho_2 g_z (h_2 - z). \tag{21}$$

It can be shown that the normal stress jump predicted by Eq. (8) is negligible under these assumptions [27]. Differently from the SH theory, we adopt an isotropic pressure distribution, i.e. $t_{\alpha,xx}(z) = t_{\alpha,zz}(z)$, for sake of simplicity. Following the same assumptions, the DBCs at Γ, (16)-(17), are recast as

$$t_{1,xz,\Gamma} = \mathrm{sgn}(\Delta v_x)\left[k(-t_{1,zz}) \tan\varphi_{\mathrm{int}} + c\rho_2 (v_{1,x} - v_{2,x})^2 \right] \tag{22}$$

$$t_{2,xz,\Gamma} = \mathrm{sgn}(\Delta v_x)(-t_{2,zz}) \tan\varphi_{\mathrm{int}}. \tag{23}$$

Besides, the assumption of shallowness leads to $|\nabla F_\Gamma| \approx 1$. Thanks to the above-mentioned hypotheses and by assuming also that the velocity distribution is blunt within each layer, we obtain the following hyperbolic partial differential equation (PDE) system

$$\begin{cases} \partial_t h_1 + \partial_x \left(\overline{v_{1,x}} h_1 \right) = \dfrac{M_{flux}}{\rho_1}, \\ \partial_t \left(\overline{v_{1,x}} h_1 \right) + \partial_x \left(\overline{v_{1,x}^2} h_1 + \dfrac{1}{2} g_z h_1^2 \right) = \\ \qquad g_x h_1 - g_z h_1 \partial_x h_2 + \overline{v_{1,x}} \dfrac{M_{flux}}{\rho_1} - \dfrac{t_{1,xz,\Gamma}}{\rho_1}, \\ \partial_t h_2 + \partial_x \left(\overline{v_{2,x}} h_2 \right) = -\dfrac{M_{flux}}{\rho_2}, \\ \partial_t \left(\overline{v_{2,x}} h_2 \right) + \partial_x \left(\overline{v_{2,x}^2} h_2 + \dfrac{1}{2} g_z h_2^2 \right) = \\ \qquad g_x h_2 - g_z \dfrac{\rho_1}{\rho_2} h_2 \partial_x h_1 - \overline{v_{2,x}} \dfrac{M_{flux}}{\rho_2} + \dfrac{t_{2,xz,\Gamma}}{\rho_2} - \dfrac{t_{2,xz,0}}{\rho_2}, \end{cases} \tag{24}$$

that is equipped with the following closure equation,

$$M_{flux} = \left(t_{1,xz} - t_{2,xz} \right) \Big/ \left(\overline{v_{1,x}} - \overline{v_{2,x}} \right). \tag{25}$$

The vector of unknowns is $\boldsymbol{q} = \left(h_1, h_1 \overline{v_{1,x}}, h_2, h_2 \overline{v_{2,x}} \right)^T$, while the advective flux vector can be written as $\boldsymbol{f}(\boldsymbol{q}) = \left(h_1 \overline{v_{1,x}}, g_z/2\, h_1^2 + h_1 \overline{v_{1,x}}^2, h_2 \overline{v_{2,x}}, g_z/2\, h_2^2 + h_2 \overline{v_{2,x}}^2 \right)^T$

It is well-known that non-conservative terms in Syst. (24), $g_z h_1 \partial_x h_2$ and $g_z (\rho_1/\rho_2) h_2 \partial_x h_1$, influence the wave celerities and make the System be only conditionally hyperbolic. The loss of hyperbolicity typically occurs in presence of large relative velocity between the layers (e.g. [6]). The source terms are composed of two parts: the mass flux term, $\boldsymbol{s}_M$, plus a remaining term due to momentum fluxes, $\boldsymbol{s}_R$,

$$\mathbf{s}_M = \left(M_{flux}/\rho_1, 0, -M_{flux}/\rho_2, 0 \right)^T, \tag{26}$$

$$\mathbf{s}_R = \begin{pmatrix} 0, g_x h_1 + \overline{v_{1,x}}\, M_{flux}/\rho_1 - t_{1,xz,\Gamma}/\rho_1, 0, g_x h_2 \\ -\overline{v_{2,x}}\, M_{flux}/\rho_2 + t_{2,xz,\Gamma}/\rho_2 - t_{2,xz,0}/\rho_2 \end{pmatrix}^T. \tag{27}$$

Thus, Syst. (24) can be rewritten in the following compact quasi-linear form

$$\partial_t \boldsymbol{q} + \partial_q \boldsymbol{f}^* \partial_x \boldsymbol{q} = \boldsymbol{s}_M + \boldsymbol{s}_R, \tag{28}$$

where $\partial_q \boldsymbol{f}^*$ represents a pseudo-Jacobian matrix of the flux vector that also takes into account the non-conservative terms (e.g. [27]).

4. Numerical scheme

The PDE system (24) together with the closure Eq. (25) is numerically integrated by a finite volume scheme. Since the PDE system exhibits non-null source terms, the operator splitting technique (e.g. [17]) is used for taking into account separately the effects of source terms. The numerical algorithm is composed of several stages. At the first stage, to calculate the effect of advection terms, the associated homogeneous PDE system,

$$\partial_t \boldsymbol{q} + \partial_q \boldsymbol{f}^* \partial_x \boldsymbol{q} = \boldsymbol{0}, \tag{29}$$

is numerically solved by using the scheme proposed by Fraccarollo et al. [11], featuring a lateralized version of the HLL approximate Riemann solver. Then, the following ordinary differential system (*ODE*),

$$d\boldsymbol{q}/dt = \boldsymbol{s}_M + \boldsymbol{s}_R, \quad \boldsymbol{q}(0) = \boldsymbol{q}^{PDE}, \tag{30}$$

is solved, by using as initial condition the solution coming from the first stage (29), detonated by the superscript *PDE*. By following the same approach of [8], two sub-steps are carried out to solve numerically Eq. (30). In the first sub-step, denoted with superscript ', the effects of the mass flux on the flow depth are explicitly calculated through the following formula,

$$(h_\alpha)_i^{'} = (h_\alpha)_i^{PDE} - \Delta t (-1)^\alpha M_{flux}/\rho_\alpha, \quad \alpha \in \{1, 2\}, \tag{31}$$

where the subscript i represents the i-th discretized cell of the spatial domain and Δt is the time step. In Eq. (31) M_{flux} is properly limited to avoid

ISBN: 978-960-474-376-6

overshooting the equilibrium flow depths or negative values of flow depths [27]. The second sub-step, denoted by the superscript ", is for calculating the effects due the momentum exchanges, $\boldsymbol{s}_R$. As friction terms in $\mathbf{s}_R$ may be very large, it is convenient to treat them in an implicit fashion (backward Euler scheme). We use as initial condition the solution obtained from the previous sub-step. The updating formula reads as follows

$$\boldsymbol{q}_i^{"} = \boldsymbol{q}_i^{'} + \Delta t\, \boldsymbol{s}_{R,i}^{"} \ . \quad (32)$$

A third stage consists of checking the system hyperbolicity by calculating numerically the eigenvalues of $\partial_{\boldsymbol{q}} \boldsymbol{f}^*$. If the two inner eigenvalues, λ_2 and λ_3, are complex conjugate numbers, which means a local loss of hyperbolicity, an additional computation stage is carried out, consisting of modifying the source terms of the momentum equations. Such a treatment is conceptually similar to the approach proposed by [7]. In particular, the algorithm comes back iteratively to the previous stage, with the following modification of the source terms

$$\boldsymbol{q}_i^{"} = \boldsymbol{q}_i^{'} + \Delta t\, \boldsymbol{s}_{R,i}^{"} + \Delta t\left(0, -F_{extra}/\rho_1, 0,\ F_{extra}/\rho_2\right)^T . \quad (33)$$

F_{extra} serves as correcting momentum flux for ensuring the numerical solution within the hyperbolicity domain. Once the new solution $\boldsymbol{q}^{"}$ is obtained, the hyperbolicity check is further performed. The amount of F_{extra} is iteratively adjusted until the solution fulfills the hyperbolicity condition. As a convergence criterion, the following expression, depending on the inner eigenvalues of $\partial_{\boldsymbol{q}} \boldsymbol{f}^*$, is used

$$\lambda_3 - \lambda_2 \le w\,, \quad (34)$$

where w is a small threshold value. At the end of this step, the variables are finally updated. Because the advective step of the numerical scheme is of explicit kind, the only constraint for time advancing is that the Courant-Friedrichs-Levy (CFL) number is smaller than 1. The proposed correction for ensuring hyperbolicity should not be regarded as a merely numerical expedient, as it locally modifies the source terms of the mathematical PDE model. Moreover, this treatment is found to have a very good stability and nice properties. A first advantage is that the correction only acts locally in space and time. Moreover, the correction does not modify the momentum balance of the layers as a whole, since it only reduces the relative velocity difference between two layers at the prediction stage.

5. Tests

5.1 Dam-break flow

Firstly, a dam-break flow of dry granular material is here reproduced by the two-layer model. The purpose of this test is to show the main features of the proposed two-layer model and its advantages over classical single layer models. The geometry of initial deposit is rectangular with a longitudinal span, L_0, equal to 1m and an initial height, $H_0 = 2\text{m}$. The channel slope is null.

The numerical results by the two-layer model are compared with those ones obtained by the single layer model, employed in [20] and featuring a purely Coulomb friction basal stress and isotropy of normal stresses. The single layer model is numerically integrated by using a finite volume scheme with the HLL approximate Riemann solver and the basal angle of friction in it is set equal to 30°.

The initial distribution of the flow depths in the two-layer model is chosen so that the lower layer consists of a wedge with an angle of $\pi/4 + \varphi_{\text{int}}$ (i.e. the angle of Rankine active state) with the horizontal. This assumption for the initial flow depth of the surface flow is quite common in Literature (e.g. [31]). The initial distributions of flow depths in both models are reported in Fig. 2. For comparison purposes, the internal angle of friction in the two-layer model is chosen equal to 30°. All the model parameters are reported in Table 1. The supposed density ratio between the layers, $\rho_1/\rho_2 = 0.67$, is reasonable in dense-collisional granular flows [27]. A study on the sensitivity of the model parameters, which is beyond the scope of this short paper, is reported in [25] and [27]. Both numerical simulations are performed over a spatial domain spanning 7m with a discretization, $\Delta x = 0.05\text{m}$. The Courant-Friedrichs-Levy (CFL) number is set equal to 0.3 for determining the time interval at each time advancing.

Table 1

φ_B	φ_{int}	k	c	ρ_1	ρ_2
40°	30°	0.97	0.1	0.4	0.6

The evolution of flow depths and flow velocities, together with the extra momentum correction, F_{extra}, at the interface, are reported in Figs. 3-4-5-6. As one can see from Figs. 3-4, while the initial spreading of granular mass is quite similar in both models up to t=0.25s, in short time the flow velocity at the front

ISBN: 978-960-474-376-6

of the dam-break wave in the single layer model becomes noticeably larger than the ones of the two-layer model. This causes a growing discrepancy between the two models as regards the positions of the front waves (see Figs. 5-6). As one can see from Fig. 7, where the final deposits are reported, the run-out distances are different with a significant overestimation by the single layer model. This result is very interesting, whereas both models employ the same angle of internal friction. As regards the dynamics of the two-layer model, it should be noted that the two layers exhibit very different dynamical behaviours. In particular, the lower layer presents significantly smaller flow velocities and reaches a state of rest at around t=0.7s while the upper surface flow is still moving and stops just before t=1.5s. This behaviour is qualitatively congruent with several experimental findings (e.g., [14,15]), where an upper highly sheared surface flow is superimposed upon a lower creep flow. The fact that such a lower wedge of granular material moves noticeably slower than the upper surface flow could explain why classical depth-averaged models are not capable to correctly predict the run-out distances of granular collapses at different initial aspect ratios, if employing a unique basal friction angle [20,28].

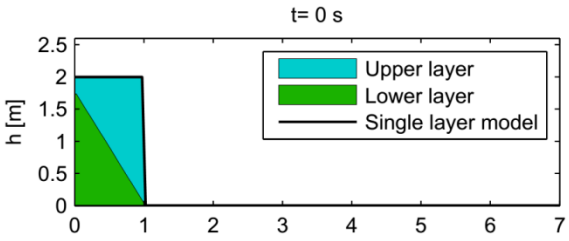

Fig.2 Initial condition for the dam-break test.

Another important aspect of the two-layer model is the capability to reproduce, at least qualitatively, the progressivity of the deposition process experienced by the granular material. Indeed, a continuous mass flux from the upper layer to the lower one takes place during the whole deposition process, thanks to the assumptions made on the non-material interface. As regards the momentum correction to preserve hyperbolicity, it should be noted from Figs. 3-6 that F_{extra} mainly acts near the front of the lower layer wave, while is null in all the other computational cells. The normalized momentum correction, F_{extra}/ρ_1, is found to be always smaller than $2\,\mathrm{m}^2/\mathrm{s}^2$ and, thus, of the same order of the interface Coulomb friction shear stress (cf Eq. (23)), if we consider that the upper layer flow depth ranges between 0.2m and 1m during almost the whole simulation.

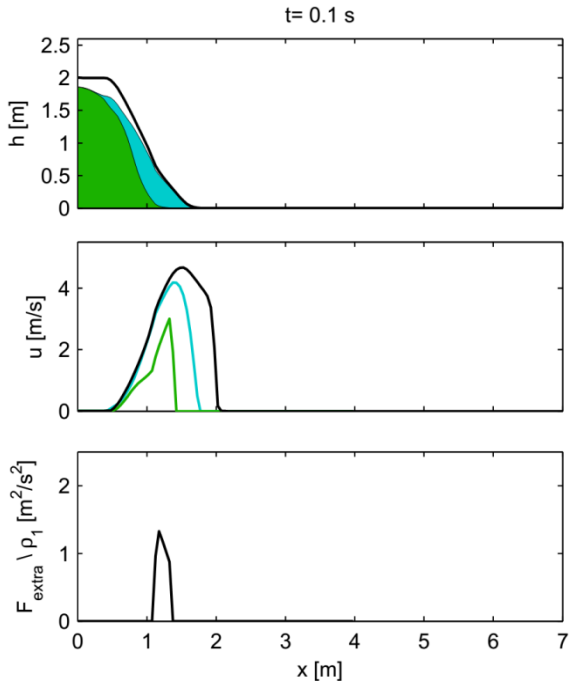

Fig.3 Evolution of flow depths (upper panel), flow velocities (middle panel) and extra momentum correction (lower panel) at t =0.1s. Black lines in the flow depth and flow velocity plots refer to the single layer model.

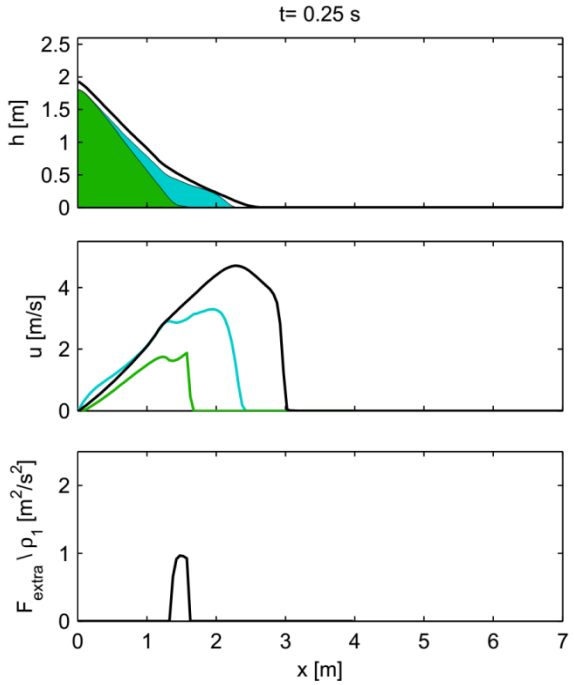

Fig.4 Evolution of flow depths (upper panel), flow velocities (middle panel) and extra momentum correction (lower panel) at t =0.25s.

ISBN: 978-960-474-376-6

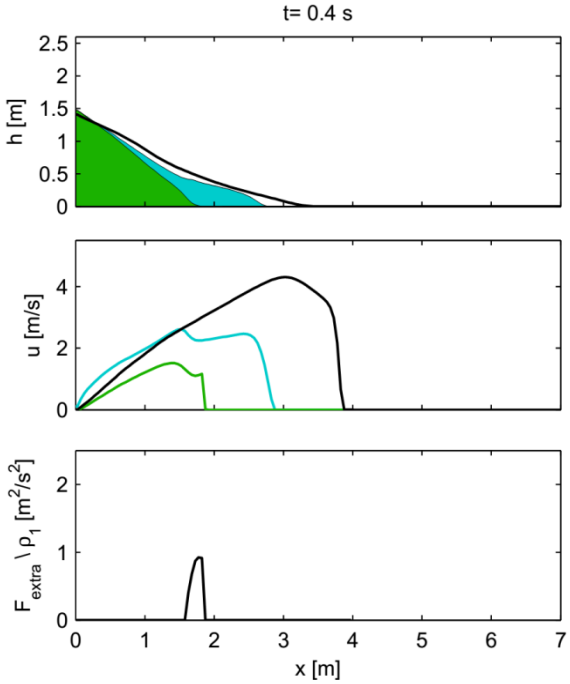

Fig.5 Evolution of flow depths (upper panel), flow velocities (middle panel) and extra momentum correction (lower panel) at t =0.4s.

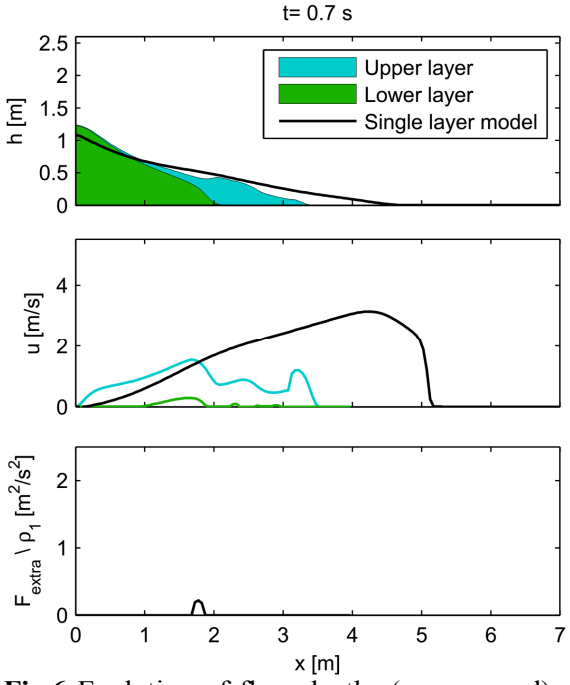

Fig.6 Evolution of flow depths (upper panel), flow velocities (middle panel) and extra momentum correction (lower panel) at t =0.7s.

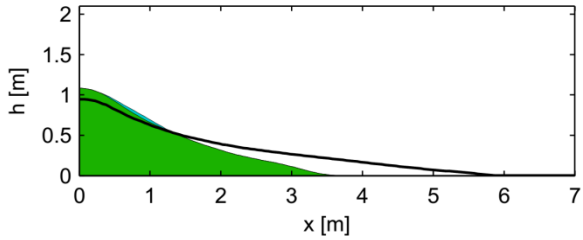

Fig.7 Final deposit at t =1.5s.

5.2 2D collapse of granular material at different initial aspect ratios

Lacaze et al. [15] reproduced two-dimensional collapses of granular columns with different initial aspect ratios, through using discrete element simulations (DEM). An interesting advantage of DEM models consists of gaining insight into phenomena impossible to be observed in real experimental cases. For instance, dam-break flows and two-dimensional collapses in real channels are always more or less influenced by the side wall friction. For this reason, a direct comparison with mathematical models would be very difficult without calibrating additional friction parameters through back-analysis. In the case of no side wall friction, Lacaze et al. [15] found that the normalized run-out distance $(R_\infty - L_0)/L_0$, scales as follows

$$r_\infty = (R_\infty - L_0)/L_0 \propto a^{0.83\pm0.03}, \qquad (35)$$

with R_∞ being the final run-out distance, L_0 the longitudinal span and $a = H_0/L_0$ the initial aspect ratio of the granular column. Here, we compare the run-out distances obtained by the proposed two-layer model with those obtained by the single layer model in case of different initial aspect ratios. The initial span of granular column is set equal to $L_0 = 0.1\text{m}$ for all simulations, while the initial height H_0 is let vary between 0.2m and 3m. All numerical simulations are performed on a spatial domain with a discretization equal to $\Delta x = 0.01\text{m}$. The basal friction angle in the single layer model has been chosen equal to 30°. The model parameters for the two-layer model are the same of the previous numerical test (cf. Table 1).

The plots of the normalized run-out distances, r_∞ , as function of the initial aspect ratio, a , are reported in logarithmic scale in Fig. 8. As one can see from Fig. 8, the single-layer is capable to reproduce quite well the run-out distances for low values of initial aspect ratios. Nevertheless, the model exhibits an almost linear dependence between r_∞ and a with a fitting curve, $r_\infty = 2.25a^{1.06}$, that causes an increasing disagreement with run-out distances predicted by

ISBN: 978-960-474-376-6

DEM simulations in [15]. Conversely, the two-layer model yields a good agreement with the scaling obtained by [15], Eq. (35), with a fitting curve $r_\infty = 1.61a^{0.84}$. It should be noted that friction angles in the mathematical model have not been calibrated on this particular dataset and, thus, the run-out distances are overall slightly underestimated. Similar scalings for the run-out distances are found by varying the friction angles.

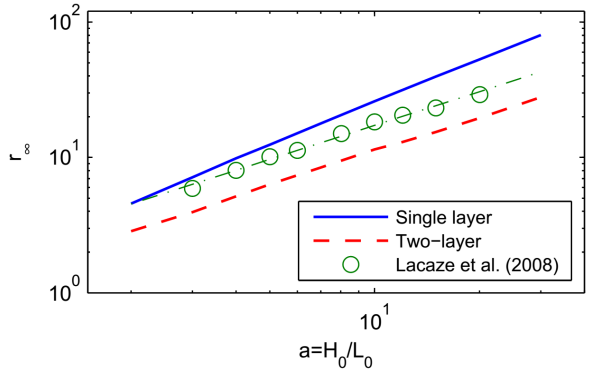

Fig.8 Normalized run-out distances r_∞ as function of the initial aspect ratio a. The fitting curves are $r_\infty = 2.25a^{1.06}$ and $r_\infty = 1.61a^{0.84}$ for single- and two-layer model, respectively.

6. Conclusion

A two-layer depth-averaged approach is proposed in order to better describe the dynamics of granular avalanches over rough bed. The flow is regarded as composed of two flowing layers, sharply separated by a non-material surface across which mass exchanges are allowed. The upper layer rheology is supposed to be of Voellmy type and, thus, exhibits a shear stress at the interface, composed of a friction term and a collisional term. Conversely, the lower layer is supposed to be purely frictional. These modelling choices are supported by several experimental investigations, where a fast surface flow is found to be superimposed on a lower creep flow. The closure equation to calculate the mass exchange between the layers is directly derived by the Rankine-Hugoniot jump conditions. The advantage of this kind of closure equation is that it uniquely depends on the rheology chosen for the flowing layers and, thus, no *ad-hoc* calibration of additional parameters is needed. The numerical finite volume scheme to solve the two-layer model uses an HLL approximate Riemann solver for accounting the advective effects and treats the source terms in a splitted fashion. Since the PDE system is conditionally hyperbolic, an additional stage, consisting of injecting an extra momentum flux at the interface is added to the numerical code. This correction is found to be very robust and yields reliable results, as shown in numerical tests. The numerical investigation on the two-layer model showed that it has several advantages over classical single layer models. At first, a better insight in the flow velocity distribution is possible thanks to intrinsically increased level of accuracy. Secondly, the two-layer approach allows to realistically describe the progressivity of the deposition stages. A further comparison with the run-out distances predicted by some DEM numerical simulations showed the capability of the two-layer model to capture the power law, describing the run-out distances as function of initial aspect ratio, in two-dimensional collapses of granular material. This represents another interesting advantage over since single layer models.

References:

[1] A. Armanini, H. Capart, L. Fraccarollo, M. Larcher, Rheological stratification in experimental free-surface flows of granular-liquid mixtures, *J. Fluid Mech.*, Vol. 532, 2005, pp. 269-319.

[2] E. Audusse, A multilayer Saint-Venant model: derivation and numerical validation, *Discrete Contin. Syst. Ser. B*, Vol. 5(2), 2005, pp. 189-214.

[3] A. Canestrelli, S. Fagherazzi and S. Lanzoni, A mass-conservative centered finite volume model for solving two-dimensional two-layer shallow water equations for fluid mud propagation over varying topography and dry areas, *Adv. Water Res.*, Vol. 40, 2012, pp. 54–70.

[4] A. Cantelli, Uniform flow of modified Bingham fluids in narrow cross sections, *J. Hydraul. Eng.*, Vol 135 No. 8, 2009, pp. 640–650.

[5] A. Carravetta, O. Fecarotta, R. Martino, C. Sabatino, Assessment of rheological characteristics of a natural Bingham-plastic mixture in turbulent pipe flow. *J. Hydraul. Eng.*, Vol. 136 No. 10, 2010, pp. 820–825.

[6] M. J. Castro, J.-A. García-Rodríguez, J. M. González-Vida, J. Marcías, C. Parés, M. E. Vásquez-Cendón, Numerical simulation of two-layer Shallow Water flows through channels with irregular geometry, *J. Comput. Phys*, Vol. 195 No. 1, 2004, pp. 202- 235.

[7] M. J. Castro-Dìaz, E. D. Fernandez-Nieto, J. M. Gonzalez-Vida, C. Parés-Madronal, Numerical Treatment of the Loss of Hyperbolicity of the Two-Layer Shallow-Water System. *J. Sci. Comput.*, Vol. 48, 2011, pp. 16-40.

[8] S.-C. Chen, S.-H. Peng and H. Capart, Two-layer shallow water computation of mud flow intrusions into quiescent water, *J. Hydr. Res.*, Vol. 45, n.1, 2007, pp. 13-25.

[9] T. G. Drake, Structural features in granular flows, *J. Geophys. Res.*, Vol. 95(B6), 1990, pp. 8681-8696.

[10] L. Fraccarollo, H. Capart, Riemann wave description of erosional dam-break flows, *J. Fluid Mech.*, Vol. 461, 2002, pp. 183-228.

[11] L. Fraccarollo, H. Capart and Y. Zech, A Godunov method for the computation of erosional shallow water transients, *Int. J. Numer. Meth. Fluids*, Vol. 41, 2003, pp. 951-976.

[12] K. Hutter, Y. Wang, S. P. Pudasaini, The Savage-Hutter avalanche model: how far can it be pushed?, *Phil. Trans. R. Soc.*, 2005, Vol. 363, pp. 1507-1528.

[13] R. M. Iverson, The physics of debris flows, *Rev. Geophys.*, Vol. 35 (3), 1997, pp. 245-296.

[14] T. Komatsu, S. Inagaki, N. Nakagawa and S. Nasuno, Creep Motion in a Granular Pile Exhibiting Steady Surface Flow, *Phys. Rev. Lett.*, Vol 86, 2001, pp. 1757–1760.

[15] L. Lacaze, J. C. Phillips, R. R. Kerswell, Planar collapse of a granular column: Experiments and discrete element simulations. *Phys. Fluids*, Vol. 20 No. 6, 2008, 063302.

[16] E. Lajeunesse, A. Mangeney-Castelnau and J. P. Vilotte, Spreading of a granular mass on a horizontal plane, *Phys. Fluids*, Vol. 16, 2004, 2371.

[17] R. J. LeVeque, Finite-Volume methods for hyperbolic problems, 2004, Cambridge University Press.

[18] G. Lube, H. E. Huppert, R. S. J. Sparks, M. A. Hallworth, Axisymmetric collapses of granular columns, *J. Fluid Mech.*, Vol. 508, 2004, pp. 175–199.

[19] I. Luca, K. Hutter, C. Y. Kuo, Y. C . Tai, Two-layer models for shallow avalanche flows over arbitrary variable topography, *Int. J. Adv. Eng. Sci. Appl. Math.*, Vol. 1, 2009, pp. 99-121.

[20] A. Mangeney-Castelnau, F. Bouchut, J. P. Vilotte, E. Lajeunesse, A. Aubertin and M. Pirulli, On the use of Saint Venant equations to simulate the spreading of a granular mass, *J. Geophys. Res.*, Vol. 110 No. B9, 2005, B09103.

[21] R. Martino, M. N. Papa, Variable-Concentration and Boundary Effects on Debris Flow Discharge Predictions, *J. Hydraul. Eng.*, Vol. 134 No. 9, 2008, pp. 1294–1301.

[22] O. Pouliquen, Y. Forterre, Friction law for dense granular flows: application to the motion of a mass down a rough inclined plane, *J. Fluid Mech.*, Vol. 453, 2002, pp. 133-151.

[23] L. Sarno, R. Martino, M. N. Papa, M. N., Discussion of "Uniform Flow of Modified Bingham Fluids in Narrow Cross Sections" by Alessandro Cantelli, *J. Hydraul. Eng.*, Vol. 137 No. 5, 2011, pp. 621–621.

[24] L. Sarno, M. N. Papa, R. Martino, Dam-break flows of dry granular material on gentle slopes. In R. Genevois, D. L. Hamilton, A. Prestininzi (Eds.), *5th Int. Conf. on Debris-Flow Hazards Mitigation: Mechanics, Prediction and Assessment*, 2011, pp. 503–512. Università La Sapienza.

[25] L. Sarno, A. Carravetta, R. Martino, Y.-C. Tai, A two-layer approach to describe granular flows over rough surface. *The 35th National Conference on Theoretical and Applied Mechanics.*, 2011, Society of Theoretical and Applied Mechanics of the Republic of China.

[26] L. Sarno, A. Carravetta, R. Martino, Y.-C. Tai, Pressure coefficient in dam-break flows of dry granular matter. *J. Hydraul. Eng.*, Vol. 139 No. 11, 2013, pp. 1126–1133.

[27] L. Sarno, *Depth-averaged models for dry granular flows*, Ph.D. thesis, University of Napoli Federico II, Italy, 2013.

[28] L. Sarno, A. Carravetta, R. Martino, Y. C. Tai, A two-layer depth-averaged approach to describe the regime stratification in dry granular flows, *Phys. Fluids* (under revision), 2014.

[29] S. B. Savage, K. Hutter, The motion of a finite mass of granular material down a rough incline", *J. Fluid Mech.*, Vol. 199, 1989, pp. 177-215.

[30] L. Staron, E. J. Hinch, Study of the collapse of granular columns using two-dimensional discrete-grain simulation, *J. Fluid Mech.*, Vol. 545, 2005, pp. 1-27.

[31] Y. C. Tai and C. Y. Kuo, Collapses of Granular Column with Time Varying Topography, *AIP Conf. Proc.*, 2010, pp. 845–850.

[32] Y. C. Tai, C.-Y. Kuo, W. H. Hui, An alternative depth-integrated formulation for granular avalanches over temporally varying topography with small curvature, *Geophys. Astrophys. Fluid Dyn.*, Vol. 106 No. 6, 2012, pp. 596–629.

[33] G. Viccione, V. Bovolin, Simulating triggering and evolution of debris-flow with SPH, In R. Genevois, D. L. Hamilton, A. Prestininzi (Eds.), *5th Int. Conf. on Debris-Flow Hazards Mitigation: Mechanics, Prediction and Assessment*, 2011, pp. 523–532. Università La Sapienza.

[34] A. Voellmy, Uber die Zerstörungskraft von Lawinen, *Schweizerische Bauzeitung*, Vol. 73, 1955, pp. 212– 285.